Supporting Information

Computational Screening of Promising Diatomic Catalyst for CO_2 Electroreduction to Syngas

Lipan Luo, Zhou Huang and Qing Tang*

School of Chemistry and Chemical Engineering, Chongqing Key Laboratory of Theoretical and Computational Chemistry, Chongqing University, Chongqing 401331, China.

*To whom correspondence should be addressed. E-mail: qingtang@cqu.edu.cn

Table S1. Thermodynamic reactions of syngas feedstock products from HER and CO_2RR and their reduction potentials (vs. RHE).

Product	Half-cell reaction	U_e(V vs. RHE)
H_2	$2\ H^+ + 2\ e^- = \rightarrow H_2$	0
CO	$CO_2 + 2\ H^+ + 2\ e^- = \rightarrow CO + H_2O$	-0.10

Table S2. The detailed electronic energy (E_*), zero-point energy (E_{ZPE}), entropy corrections (TS), and free energy (G) of isolated molecule during electrochemical CO_2RR and HER.

Species	E_*	E_{ZPE}	TS	G
CO_2	-22.96	0.31	0.66	-23.31
CO	-14.84	0.14	0.61	-15.31
H_2O	-14.25	0.59	0.58	-14.24
H_2	-6.76	0.27	0.40	-6.89

Table S3. The detailed electronic energy (E_*), zero-point energy (E_{ZPE}), entropy corrections (TS), free energy (G), and Gibbs free energy change (ΔG) of *H intermediate on M1M2@DAC1 during electrochemical HER.

Species	E_*	E_{*H}	E_{ZPE}	TS	G	ΔG_{*H}
Cr-Mn	-438.33	-441.73	0.20	0.01	-441.54	0.24
Cr-Fe	-437.29	-440.78	0.21	0.01	-440.57	0.17
Cr-Co	-436.22	-439.07	0.21	0.01	-438.87	0.80

Cr-Ni	-434.28	-436.06	0.14	0.01	-435.93	1.80
Cr-Cu	-431.06	-432.88	0.14	0.03	-432.76	1.75
Cr-Zn	-428.62	-431.78	0.16	0.02	-431.64	0.42
Mn-Cr	-438.33	-441.96	0.20	0.01	-441.77	0.01
Mn-Fe	-436.57	-440.30	0.22	0.01	-440.09	-0.07
Mn-Co	-435.66	-438.30	0.21	0.01	-438.11	1.00
Mn-Ni	-433.43	-435.43	0.17	0.01	-435.27	1.62
Mn-Cu	-430.32	-432.13	0.14	0.02	-432.01	1.75
Fe-Cr	-437.29	-440.75	0.20	0.01	-440.56	0.18
Fe-Mn	-436.57	-439.32	0.20	0.01	-439.13	0.90
Fe-Co	-434.10	-436.67	0.20	0.01	-436.48	1.07
Fe-Zn	-426.58	-429.57	0.15	0.03	-429.45	0.58
Co-Cr	-436.22	-439.59	0.20	0.01	-439.40	0.27
Co-Mn	-435.66	-438.85	0.21	0.01	-438.65	0.46
Co-Fe	-434.10	-437.54	0.22	0.01	-437.33	0.22
Co-Ni	-430.76	-432.83	0.18	0.01	-432.66	1.55
Co-Cu	-427.61	-429.43	0.13	0.03	-429.32	1.73
Ni-Cr	-434.28	-437.66	0.20	0.01	-437.47	0.26
Ni-Mn	-433.43	-436.78	0.21	0.01	-436.58	0.30
Ni-Fe	-432.16	-435.41	0.21	0.01	-435.22	0.39
Ni-Co	-430.76	-433.80	0.21	0.01	-433.60	0.61
Ni-Cu	-426.12	-427.80	0.13	0.02	-427.70	1.87

Ni-Zn	-423.94	-426.53	0.16	0.03	-426.41	0.98
Cu-Cr	-431.06	-434.46	0.20	0.01	-434.28	0.23
Cu-Mn	-430.32	-433.43	0.21	0.01	-433.23	0.54
Cu-Fe	-429.02	-432.25	0.21	0.01	-432.06	0.41
Cu-Co	-427.61	-430.69	0.21	0.01	-430.50	0.56
Cu-Ni	-426.12	-428.46	0.19	0.01	-428.29	1.28
Cu-Zn	-421.22	-424.12	0.17	0.02	-423.96	0.71
Zn-Cr	-428.62	-432.04	0.20	0.01	-431.84	0.22
Zn-Mn	-427.99	-431.11	0.20	0.01	-430.92	0.52
Zn-Fe	-426.58	-429.91	0.20	0.01	-429.71	0.32
Zn-Co	-425.26	-428.44	0.21	0.01	-428.23	0.47
Zn-Ni	-423.94	-426.29	0.19	0.01	-426.12	1.27

Table S4. The detailed electronic energy (E_*), zero-point energy (E_{ZPE}), entropy corrections (TS), free energy (G), and Gibbs free energy change (ΔG) of *CO_2 intermediate on M1M2@DAC1 during electrochemical CO_2RR.

Species	E_{*CO2}	E_{ZPE}	TS	G	ΔG_1
Cr-Mn	-461.58	0.31	0.07	-461.35	0.09
Cr-Fe	-460.66	0.31	0.07	-460.43	-0.03
Cr-Co	-459.46	0.31	0.14	-459.29	0.04
Cr-Ni	-457.53	0.31	0.12	-457.33	0.06
Cr-Cu	-454.32	0.31	0.12	-454.13	0.04

Cr-Zn	-451.91	0.31	0.11	-451.71	0.02
Mn-Cr	-461.58	0.31	0.07	-461.35	0.09
Mn-Fe	-459.92	0.30	0.01	-459.62	0.06
Mn-Co	-458.89	0.31	0.13	-458.71	0.06
Mn-Ni	-456.66	0.31	0.07	-456.43	0.12
Mn-Cu	-453.57	0.31	0.07	-453.33	0.10
Fe-Cr	-460.41	0.31	0.07	-460.18	0.22
Fe-Mn	-460.25	0.30	0.01	-459.96	-0.27
Fe-Co	-457.47	0.31	0.11	-457.28	-0.06
Fe-Zn	-449.83	0.31	0.12	-449.64	0.05
Co-Cr	-459.48	0.31	0.07	-459.25	0.08
Co-Mn	-458.92	0.30	0.07	-458.69	0.08
Co-Fe	-457.47	0.31	0.18	-457.34	-0.13
Co-Ni	-454.03	0.31	0.18	-453.89	-0.02
Co-Cu	-450.87	0.30	0.07	-450.64	0.07
Ni-Cr	-457.54	0.31	0.13	-457.36	0.03
Ni-Mn	-456.70	0.31	0.19	-456.58	-0.03
Ni-Fe	-455.35	0.32	0.22	-455.25	0.02
Ni-Co	-454.02	0.32	0.17	-453.88	-0.01
Ni-Cu	-449.37	0.32	0.23	-449.28	-0.05
Ni-Zn	-447.22	0.32	0.18	-447.08	-0.04
Cu-Cr	-454.33	0.31	0.06	-454.07	0.10

Cu-Mn	-453.54	0.31	0.06	-453.30	0.13
Cu-Fe	-452.18	0.32	0.11	-451.97	0.16
Cu-Co	-450.85	0.31	0.13	-450.66	0.06
Cu-Ni	-449.37	0.31	0.12	-449.17	0.06
Cu-Zn	-444.43	0.31	0.12	-444.24	0.09
Zn-Cr	-451.87	0.32	0.17	-451.72	0.00
Zn-Mn	-451.25	0.31	0.12	-451.06	0.04
Zn-Fe	-449.84	0.31	0.19	-449.72	-0.02
Zn-Co	-448.54	0.32	0.16	-448.38	-0.01
Zn-Ni	-447.19	0.31	0.11	-446.99	0.05

Table S5. The detailed electronic energy (E_*), zero-point energy (E_{ZPE}), entropy corrections (TS), free energy (G), and Gibbs free energy change (ΔG) of *COOH intermediate on M1M2@DAC1 during electrochemical CO_2RR.

Species	E_{*COOH}	E_{ZPE}	TS	G	ΔG_2
Cr-Mn	-465.41	0.60	0.13	-464.94	-0.14
Cr-Fe	-464.23	0.60	0.13	-463.76	0.12
Cr-Co	-463.08	0.60	0.14	-462.62	0.12
Cr-Ni	-461.16	0.61	0.12	-460.67	0.12
Cr-Cu	-457.99	0.59	0.08	-457.47	0.11
Cr-Zn	-455.75	0.61	0.16	-455.30	-0.15
Mn-Cr	-465.18	0.60	0.07	-464.65	0.15

Mn-Fe	-463.57	0.60	0.07	-463.04	0.03
Mn-Co	-462.32	0.61	0.12	-461.84	0.33
Mn-Ni	-460.29	0.61	0.06	-459.74	0.13
Mn-Cu	-456.98	0.60	0.07	-456.45	0.33
Fe-Cr	-464.17	0.61	0.12	-463.68	-0.05
Fe-Mn	-463.87	0.62	0.12	-463.37	0.04
Fe-Co	-461.01	0.62	0.17	-460.56	0.17
Fe-Zn	-453.64	0.62	0.14	-453.15	-0.06
Co-Cr	-462.56	0.62	0.17	-462.11	0.59
Co-Mn	-461.78	0.61	0.11	-461.28	0.86
Co-Fe	-460.25	0.61	0.11	-459.75	1.04
Co-Ni	-457.30	0.62	0.16	-456.84	0.50
Co-Cu	-454.20	0.61	0.12	-453.71	0.38
Ni-Cr	-459.64	0.59	0.14	-459.19	1.62
Ni-Mn	-458.97	0.61	0.17	-458.52	1.50
Ni-Fe	-457.60	0.61	0.18	-457.17	1.53
Ni-Co	-456.36	0.61	0.18	-455.93	1.40
Ni-Cu	-451.90	0.62	0.13	-451.41	1.31
Ni-Zn	-449.75	0.61	0.18	-449.33	1.21
Cu-Cr	-456.51	0.59	0.15	-456.08	1.45
Cu-Mn	-455.73	0.58	0.09	-455.24	1.51
Cu-Fe	-454.23	0.58	0.15	-453.80	1.62

Cu-Co	-452.98	0.60	0.12	-452.51	1.60
Cu-Ni	-451.44	0.59	0.13	-450.98	1.64
Cu-Zn	-446.50	0.59	0.13	-446.04	1.65
Zn-Cr	-455.16	0.60	0.18	-454.74	0.43
Zn-Mn	-454.49	0.60	0.19	-454.08	0.43
Zn-Fe	-453.02	0.60	0.19	-452.61	0.56
Zn-Co	-451.53	0.60	0.19	-451.12	0.71
Zn-Ni	-449.92	0.59	0.13	-449.45	0.99

Table S6. The detailed electronic energy (E_*), zero-point energy (E_{ZPE}), entropy corrections (TS), free energy (G), and Gibbs free energy change (ΔG) of *CO intermediate on M1M2@DAC1 during electrochemical CO_2RR.

Species	E_{*CO}	E_{ZPE}	TS	G	ΔG_3	ΔG_4
Cr-Mn	-454.61	0.20	0.08	-454.49	-0.34	0.50
Cr-Fe	-453.19	0.20	0.09	-453.08	-0.12	0.14
Cr-Co	-452.28	0.20	0.16	-452.24	-0.41	0.37
Cr-Ni	-450.39	0.20	0.09	-450.28	-0.40	0.35
Cr-Cu	-447.23	0.19	0.04	-447.08	-0.40	0.37
Cr-Zn	-443.57	0.15	0.15	-443.57	0.94	-0.69
Mn-Cr	-453.40	0.19	0.08	-453.30	0.56	-0.68
Mn-Fe	-451.78	0.18	0.08	-451.69	0.57	-0.54
Mn-Co	-450.72	0.19	0.08	-450.61	0.44	-0.70

Mn-Ni	-448.52	0.19	0.08	-448.40	0.55	-0.68
Mn-Cu	-445.27	0.15	0.16	-445.28	0.38	-0.69
Fe-Cr	-452.22	0.16	0.23	-452.29	0.60	-0.64
Fe-Mn	-451.91	0.15	0.19	-451.95	0.63	-0.27
Fe-Co	-449.19	0.15	0.15	-449.19	0.58	-0.56
Fe-Zn	-441.53	0.14	0.15	-441.54	0.82	-0.70
Co-Cr	-451.20	0.15	0.14	-451.19	0.13	-0.68
Co-Mn	-450.63	0.15	0.14	-450.62	-0.13	-0.69
Co-Fe	-449.18	0.15	0.20	-449.23	-0.27	-0.52
Co-Ni	-445.75	0.14	0.08	-445.69	0.35	-0.71
Co-Cu	-442.59	0.15	0.14	-442.58	0.34	-0.68
Ni-Cr	-449.23	0.15	0.21	-449.29	-0.89	-0.64
Ni-Mn	-448.37	0.15	0.20	-448.42	-0.69	-0.66
Ni-Fe	-447.04	0.15	0.21	-447.10	-0.71	-0.71
Ni-Co	-445.72	0.15	0.27	-445.83	-0.69	-0.58
Ni-Cu	-441.09	0.15	0.25	-441.19	-0.57	-0.58
Ni-Zn	-438.92	0.15	0.19	-438.96	-0.43	-0.63
Cu-Cr	-446.01	0.15	0.15	-446.01	-0.72	-0.70
Cu-Mn	-445.26	0.15	0.21	-445.32	-0.88	-0.64
Cu-Fe	-443.89	0.14	0.16	-443.90	-0.89	-0.76
Cu-Co	-442.54	0.15	0.16	-442.56	-0.84	-0.70
Cu-Ni	-441.07	0.15	0.22	-441.15	-0.96	-0.62

Cu-Zn	-436.15	0.15	0.15	-436.16	-0.91	-0.71
Zn-Cr	-443.57	0.15	0.19	-443.60	0.35	-0.66
Zn-Mn	-443.06	0.17	0.08	-442.97	0.32	-0.67
Zn-Fe	-441.54	0.15	0.20	-441.59	0.23	-0.64
Zn-Co	-440.21	0.16	0.25	-440.31	0.02	-0.60
Zn-Ni	-438.99	0.18	0.17	-438.98	-0.32	-0.61

Table S7. The total energies of M1M2@DAC structures ($E_{M1M2@DAC}$) (M = Cr, Mn, or Fe), individual metal atoms in bulk form (E_{M1} and E_{M2}), and N-doped graphene substrate (E_{NC}), along with their Binding Energies (Eb).

Species	E_{M1M2}@DAC	E_{M1}	E_{M2}	E_{NC}	E_b
CrMn@DAC1	-434.75	-9.64	-9.16	-411.59	-4.36
CrFe@DAC1	-433.63	-9.64	-8.46	-411.59	-3.94
MnFe@DAC1	-433.17	-9.16	-8.46	-411.59	-3.96
CrMn@DAC2	-438.39	-9.64	-9.16	-411.56	-8.03
CrFe@DAC2	-437.40	-9.64	-8.46	-411.56	-7.74
MnFe@DAC2	-437.04	-9.16	-8.46	-411.56	-7.87
CrMn@DAC3	-434.99	-9.64	-9.16	-411.09	-5.10
CrFe@DAC3	-433.89	-9.64	-8.46	-411.09	-4.70
MnFe@DAC3	-433.41	-9.16	-8.46	-411.09	-4.70

Table S8. The total magnetization of M1M2@DAC structures ($E_{M1M2@DAC}$) (M = Cr, Mn, or Fe) and metal atom.

Species	Total magnetization	Metal atom	Total magnetization
CrMn@DAC1	3.34	Cr	1.72
		Mn	2.07
CrFe@DAC1	2.55	Cr	1.82
		Fe	1.10
MnFe@DAC1	1.32	Mn	2.41
		Fe	-0.90
CrMn@DAC2	6.29	Cr	3.39
		Mn	2.97
CrFe@DAC2	5.29	Cr	3.39
		Fe	1.83
MnFe@DAC2	4.66	Mn	3.01
		Fe	1.90
CrMn@DAC3	6.17	Cr	3.41
		Mn	2.96
CrFe@DAC3	5.19	Cr	3.42
		Fe	1.85
MnFe@DAC3	4.49	Mn	2.98
		Fe	1.81

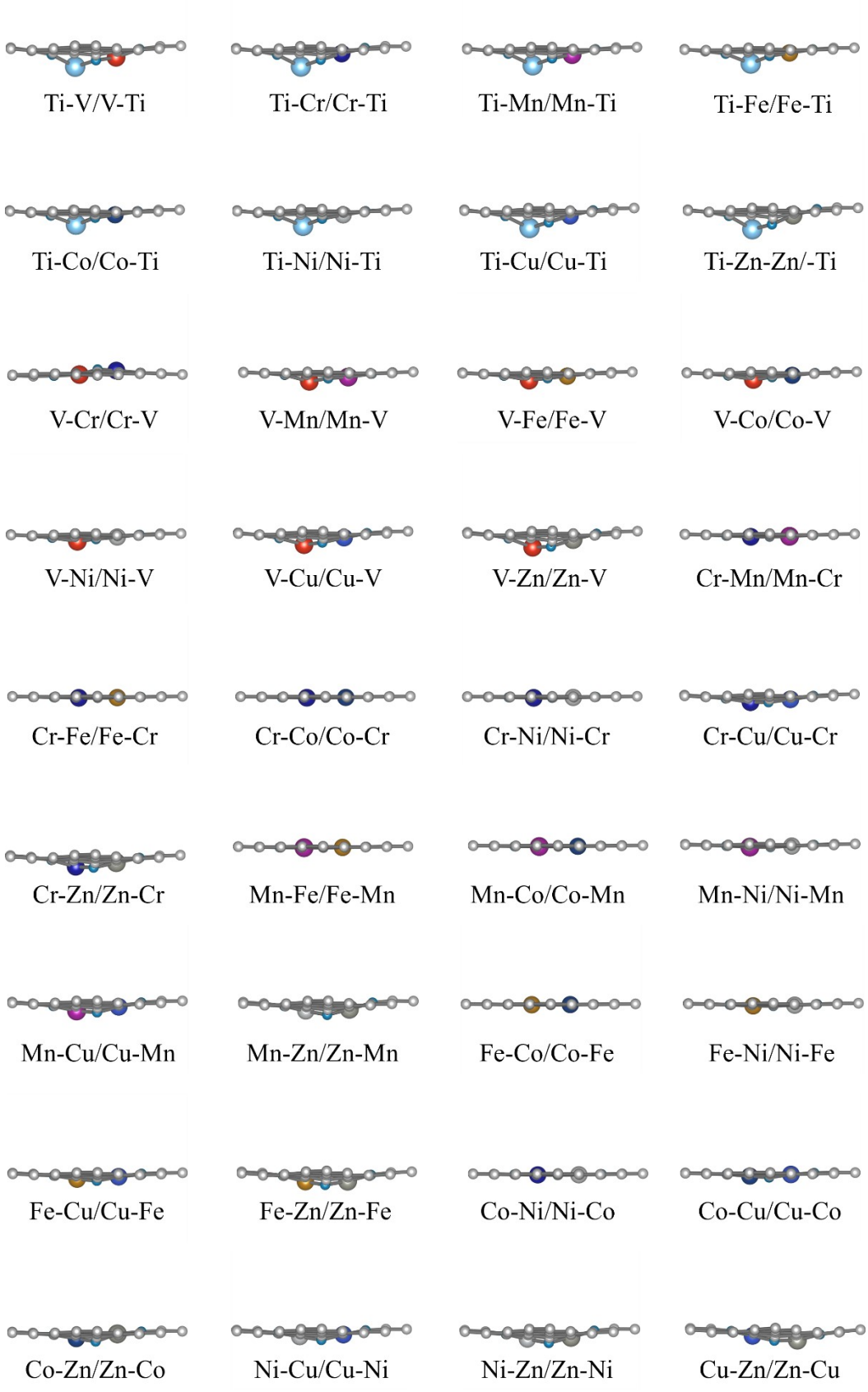

Figure S1. The side view of the optimized structures of DACs with M1M2@DAC1 configuration.

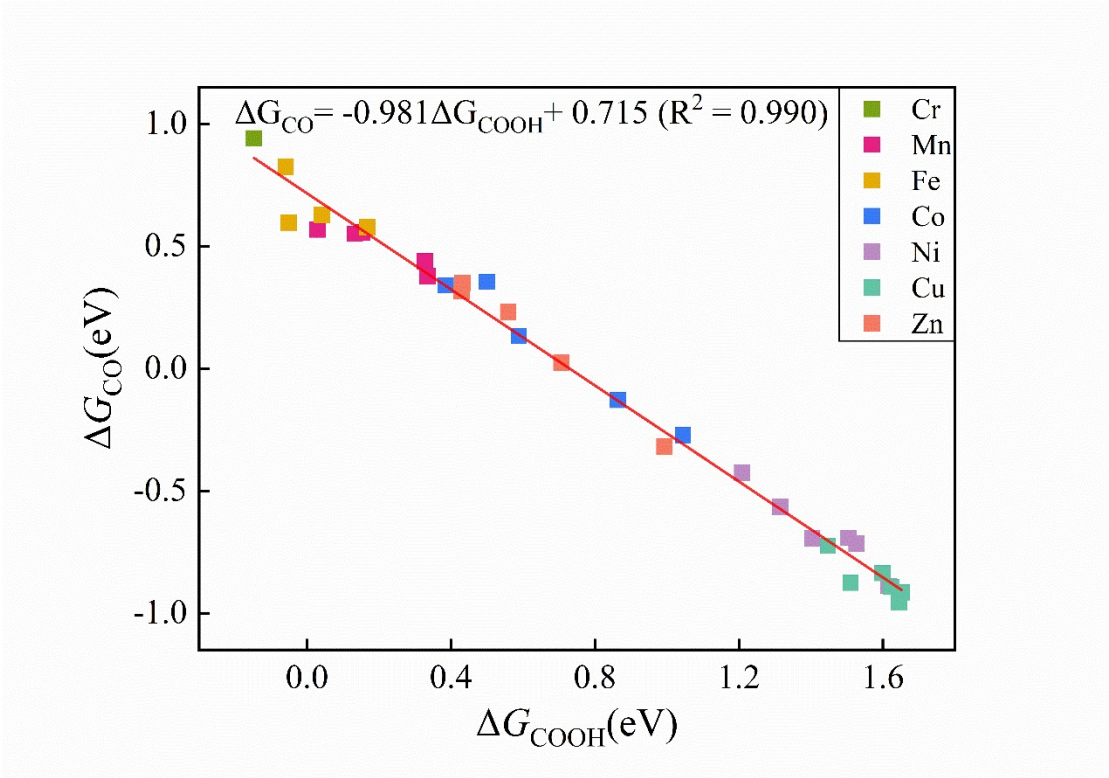

Figure S2. Refined linear scaling relations for ΔG_{COOH} and ΔG_{CO} in M1M2@DAC1, excluding outlier points from Cr-based configurations.

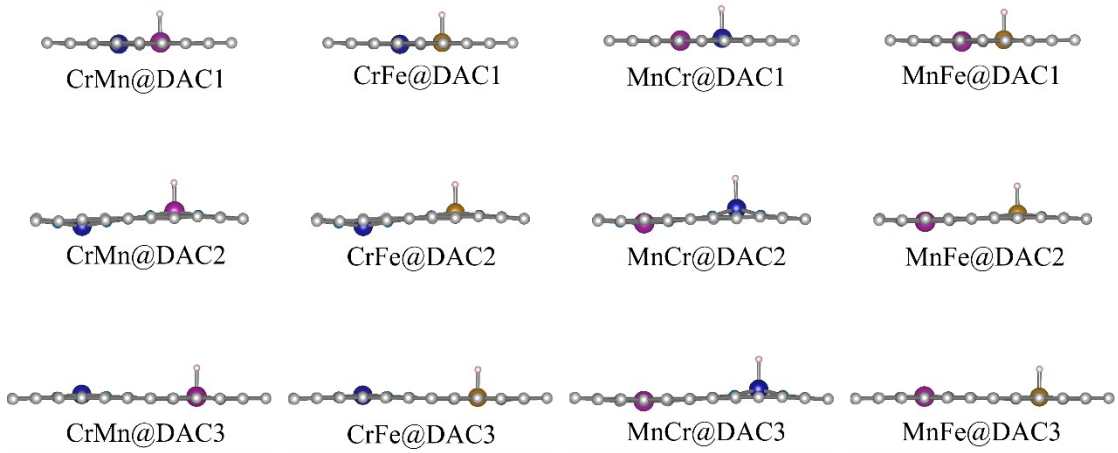

Figure S3. The most stable structures of *H adsorbed on three configurations of DACs.

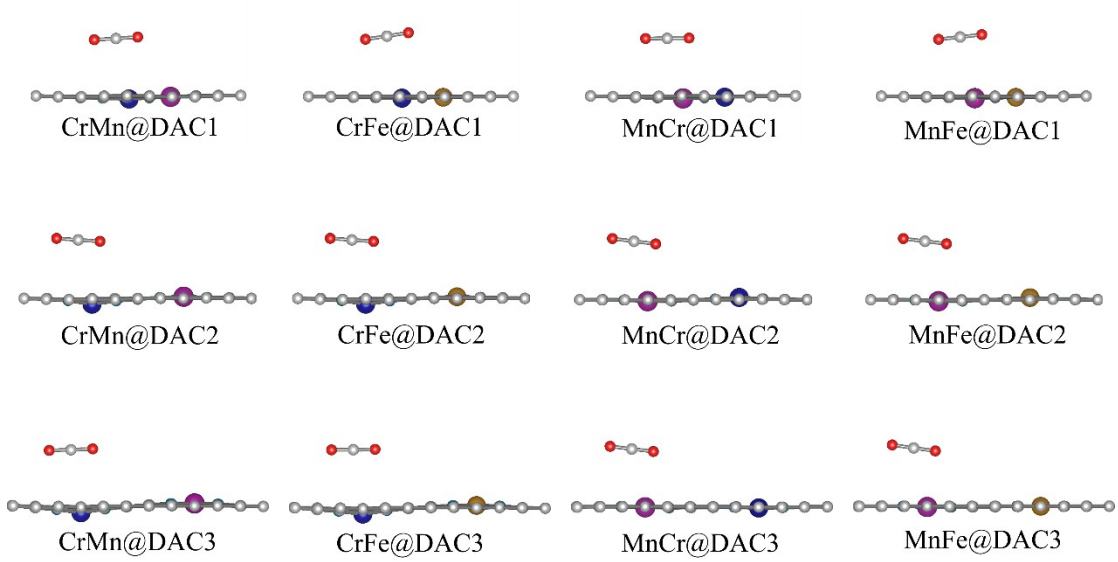

Figure S4. The most stable structures of *CO_2 adsorbed on three configurations of DACs.

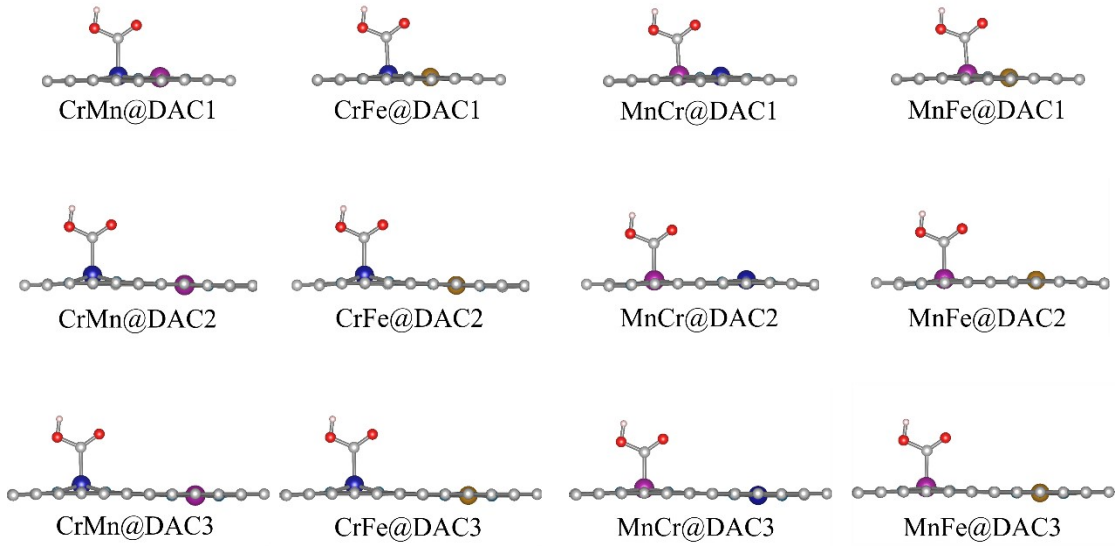

Figure S5. The most stable structures of * COOH adsorbed on three configurations of DACs.

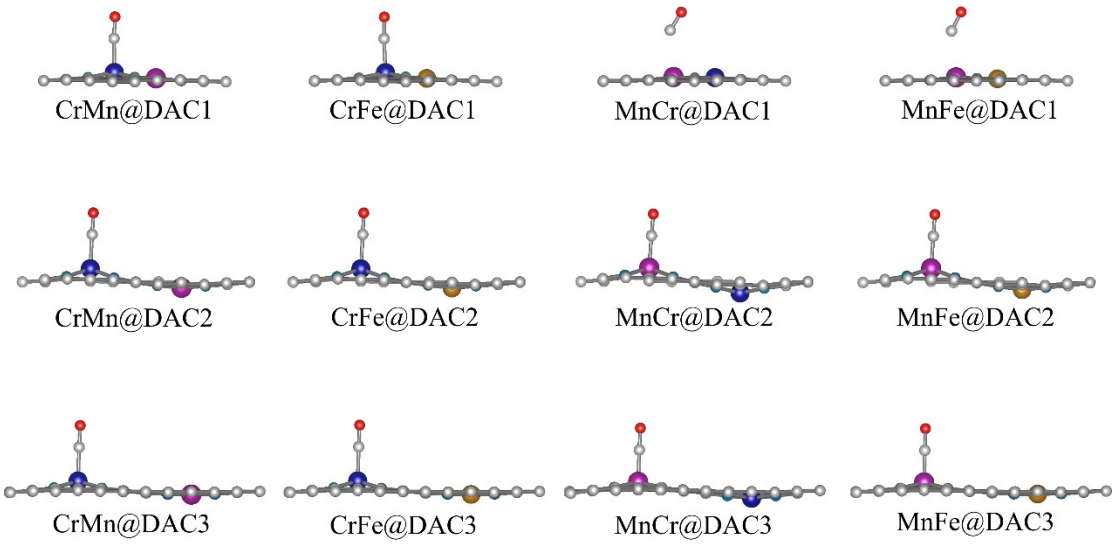

Figure S6. The most stable structures of *CO adsorbed on three configurations of DACs.

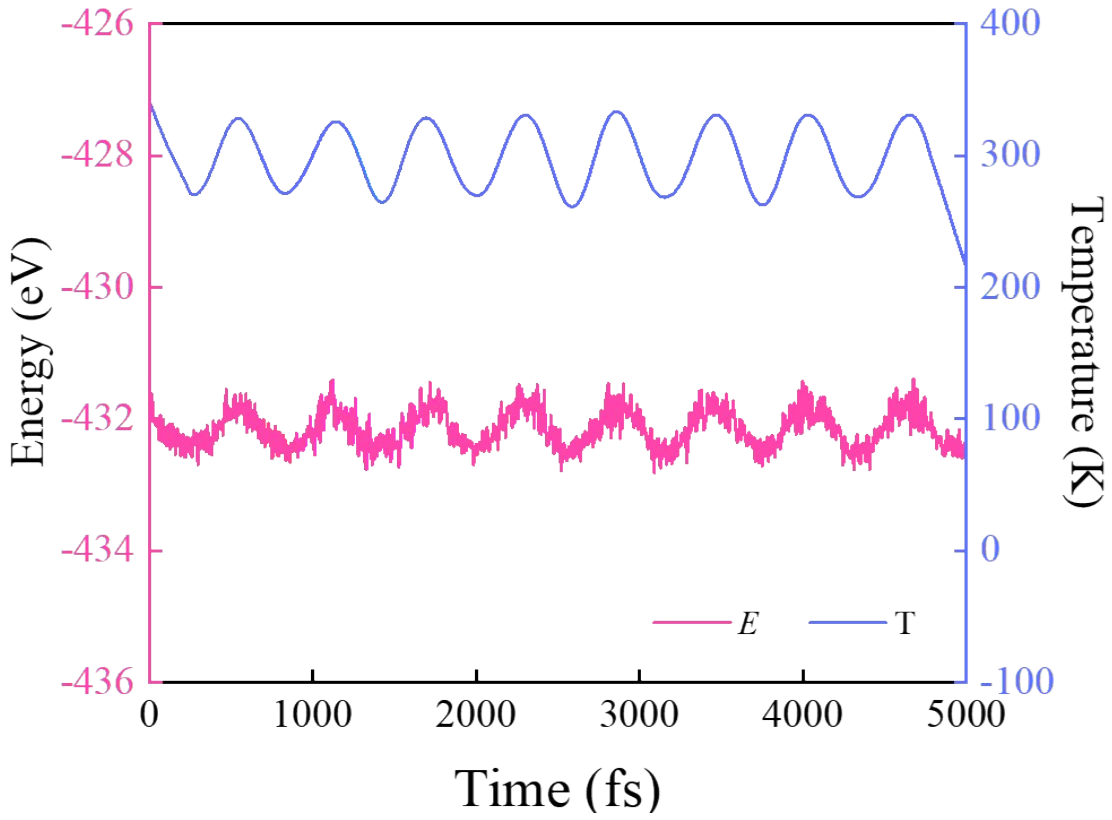

Figure S7. AIMD simulation of CrFe@DAC2 at 300K over 5 ps with a time step of 1fs.

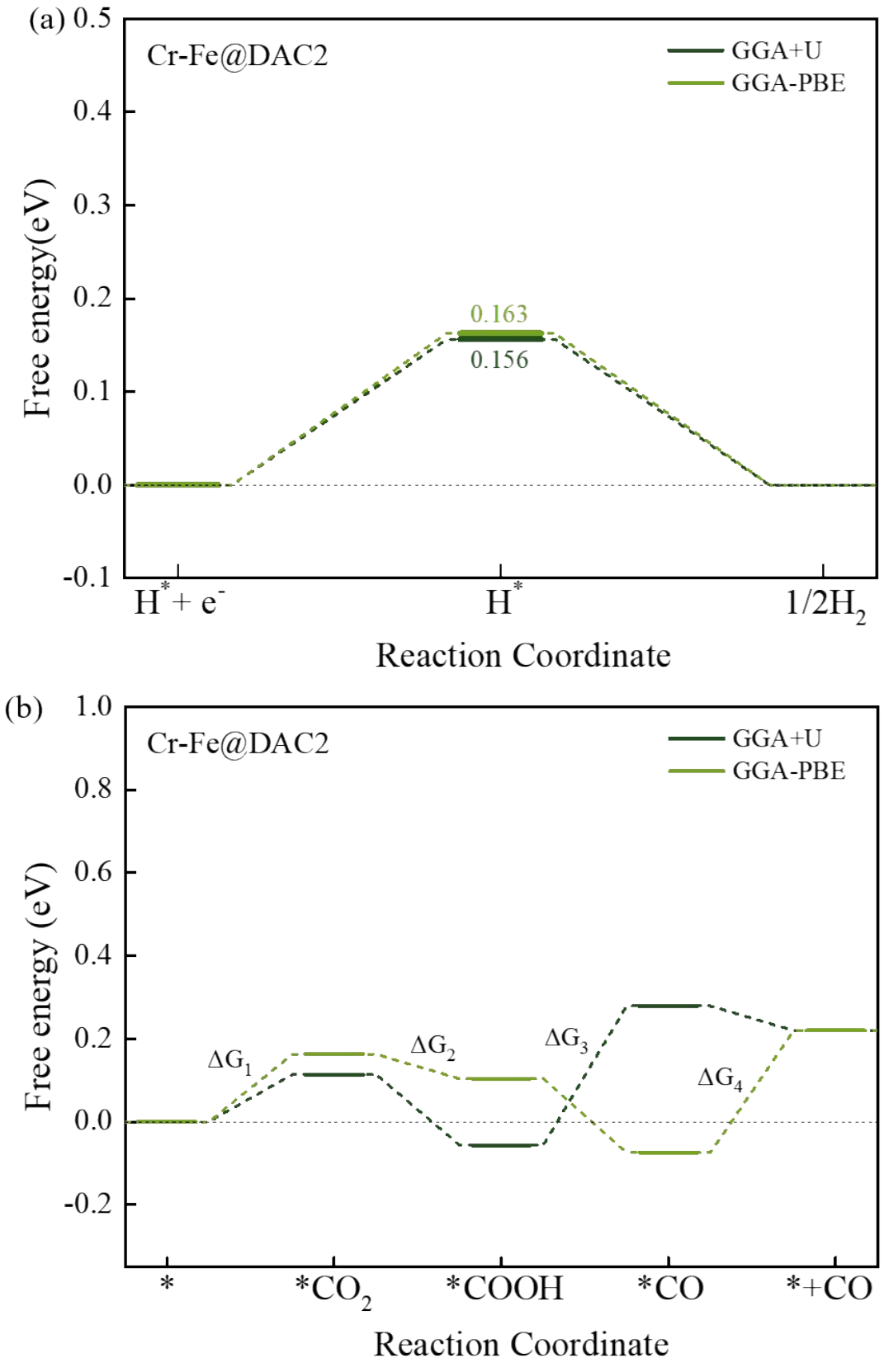

Figure S8. Comparison of free energies diagram of HER (a) and CO_2RR-to-CO (b) on CrFe@DAC2 calculated using GGA-PBE and GGA+*U* generalized functions.

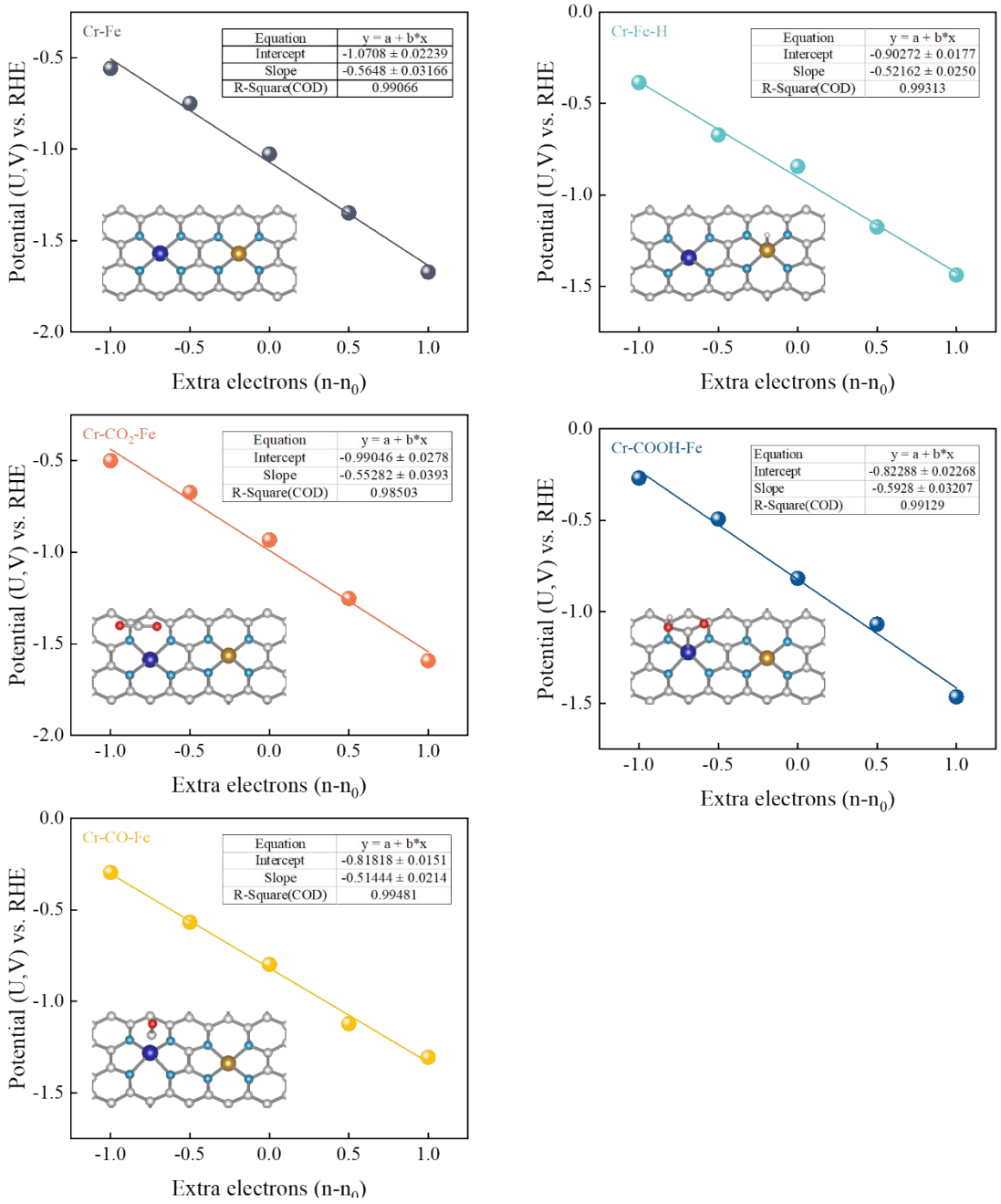

Figure S9. The relationships between the extra electrons ($n-n_0$) and the corresponded electrode potential U_{RHE} on CrFe@DAC2 and its configurations adsorbing CO_2RR-to-CO and HER intermediates.

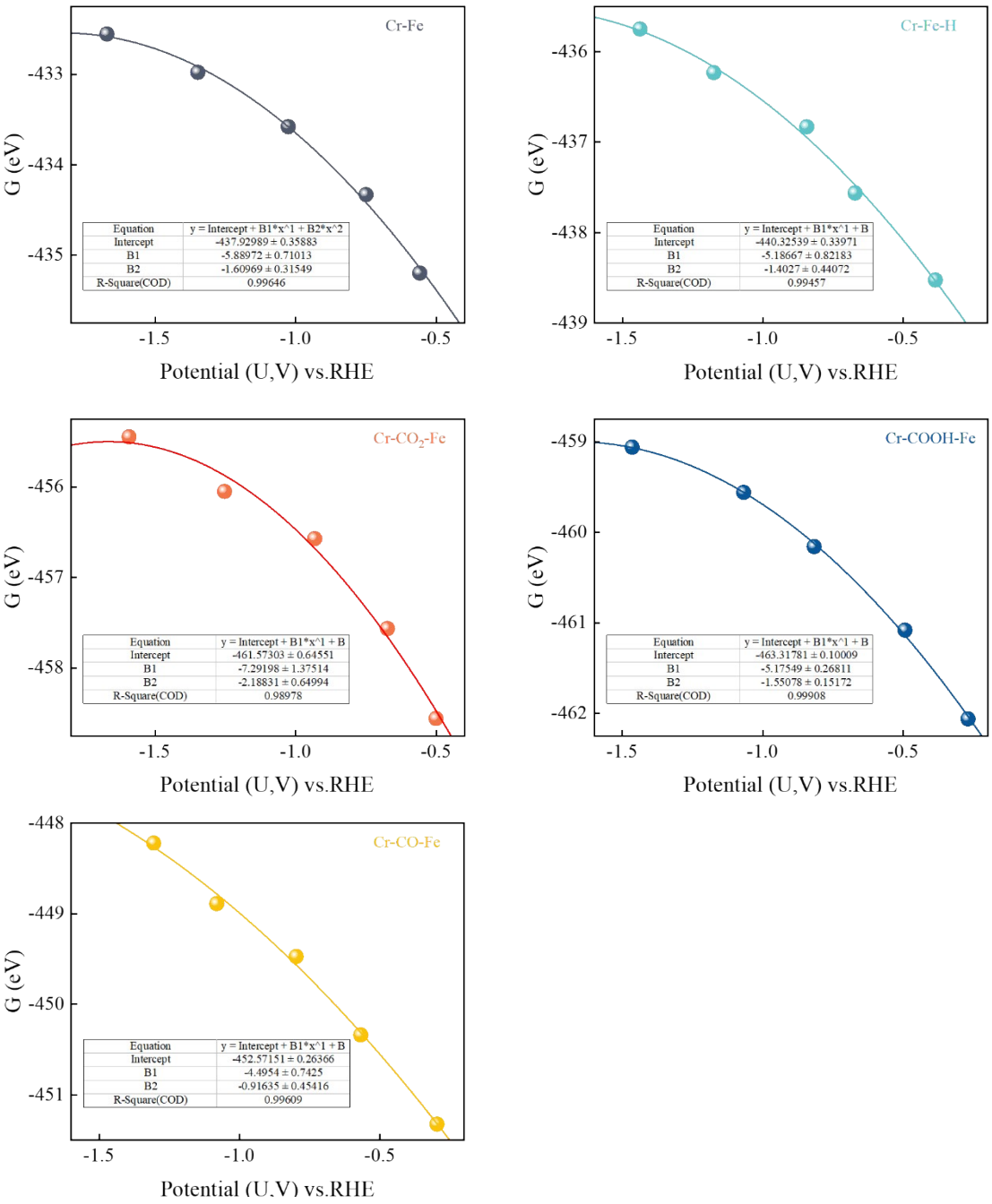

Figure S10. Free energy profiles and polynomial fits for CrFe@DAC2 in CO_2RR-to-CO and HER processes, analyzed as a function of potential U_{RHE} calculated using the constant potential method (CPM).

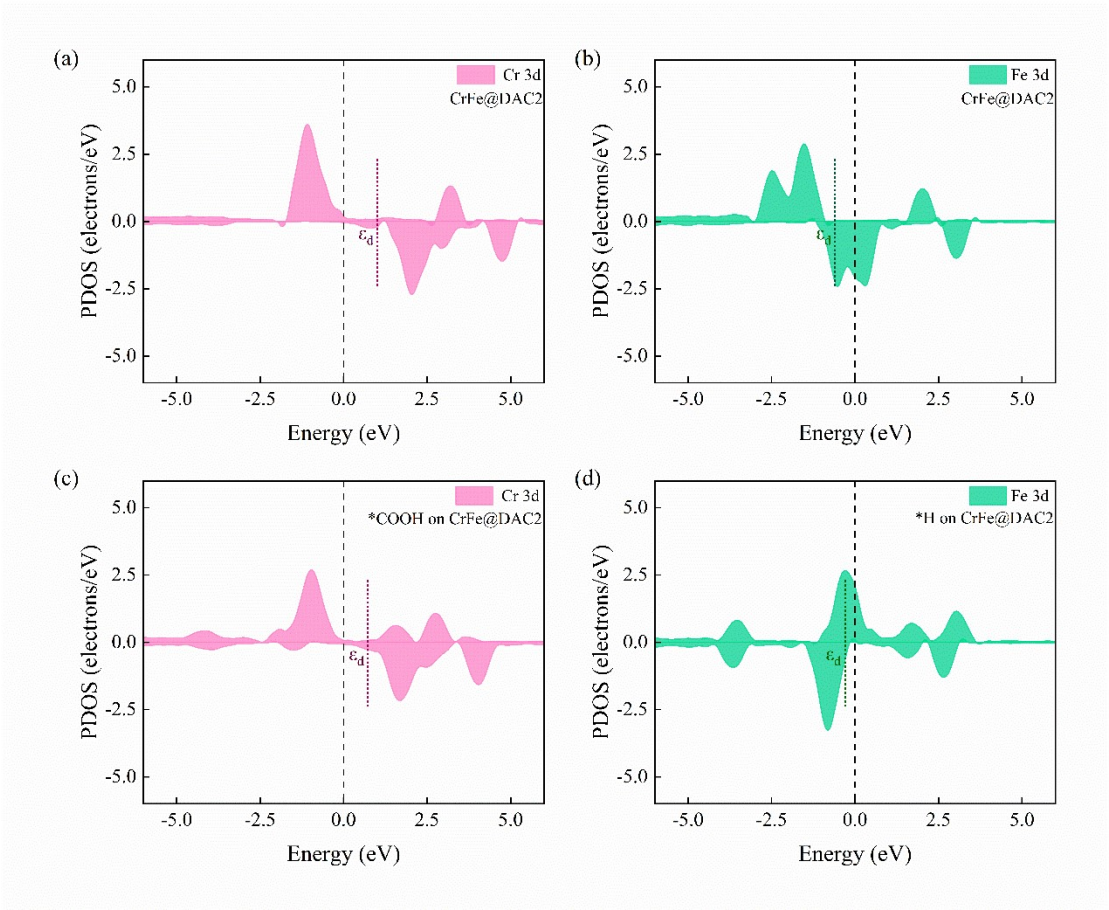

Figure S11. The PDOS and d-band-center (ε_d) of Cr and Fe atoms on the pristine CrFe@DAC2 and after adsorption of reaction intermediates.